COMPREHENSIVE DYNAMIC AND STABILITY ANALYSIS OF ELECTROSTATIC VIBRATION ENERGY HARVESTER (E-VEH)

D. Galayko[1]*, R. Guillemet*[2]*, A. Dudka*[1]*, P. Basset*[2]
[1]LIP6, UPMC Universités Paris Sorbonne, Paris, France
[2]Unversité Paris-Est, ESYCOM, ESIEE Paris, Noisy-le-Grand,France

ABSTRACT

This paper reports on an investigation of dynamic behavior of an electrostatic Vibration Energy Harvester (e-VEH) which uses gap-closing capacitive transducers and operates in a constant-charge mode. This work provides a deep insight into stability issues of a e-VEH investigating four dynamic modes, among which only one corresponds to a regular, stable and desirable operation mode needed for the energy conversion. The three other modes represent instable behavior. Each one corresponds to a particular range of external acceleration, and in none of these modes the e-VEH behaves similarly to an ideal constant-voltage biased transducer associated with a resonator. This paper describes a modeling experiment allowing a demonstration of the four operation modes, and proposes theoretical considerations for their quantitative description.

1. INTRODUCTION

One major limitation of electrostatic Vibration Energy Harvester (e-VEH) is the related (in)stability due to the presence of both mechanical and electrostatic forces. The present work addresses the problem of mechanical stability of the system "electrostatic transducer – mechanical resonator" in this particular context [1]. To date, many studies have been carried out, aiming to understand the dynamic behavior of a voltage biased electrostatic transducer associated with a mechanical resonator in applications like accelerometers, mechanical signal processing and oscillators. The main instability phenomenon related to dynamic and static pull-in has been deeply investigated for such systems [2][3]. However, in a constant-charge electrostatic harvester [4], the transducer operates in a more complex context:

- when the capacitance of the transducer increases, the transducer is biased to a zero voltage;
- when the capacitance of the transducer decreases, the transducer is biased by a constant charge Q, hence operating at a variable voltage.
- switching between these two modes is done by an external conditioning circuit which detects the local maximum and minimum on the value of the transducer capacitance C_{var}, and which controls the charge flow on the transducer.

As demonstrates our study, such a system exhibits much more complex behavior than in the case when the transducer is biased with a constant voltage. Depending on the magnitude of the external acceleration, four different operation modes are possible. Among them, only one is appropriate for efficient energy harvesting and the three other can be seen as instable behavior. In this paper we firstly present a modeling experiment demonstrating these phenomena, and then we present the theory explaining and characterizing it.

Description of the studied system and of the experiment

The modeling experiment has been carried out on a resonator described with a second-order model. The capacitive transducer has been described with a VHDL-AMS model based on the physical equations [5]. Here we consider a case of a gap-closing transducer, in which the electrodes moves in the direction perpendicular to their planes. In this case, $C_{var}(x)$ is monotonic and is expressed as:

$$C_{\mathrm{var}}(x) = \varepsilon_0 \frac{S}{d_0 - x}, \qquad (1)$$

where x is the mobile electrode (mobile mass) position, S is the overlapping electrode area, d_0 is the initial gap between the electrodes, ε_0 is the permittivity of vacuum.

The conditioning circuit used for the experiment (modeled with its electrical netlist) is given in fig.1. The purpose of this circuit is to put a charge Q on the transducer when its capacitance is maximal, and to discharge the transducer quickly when its capacitance is minimal. The switches SW1 and SW2 are driven by a min/max detection circuit measuring the transducer's capacitance (the detector is represented with a VHDL-AMS model, not shown here). The value of the charge Q put on the transducer depends on the value of the maximal capacitance C_{max} of the transducer and on the voltage U_0 of the voltage source, $Q=U_0C_{max}$. C_{max}, in turn, depends on the dynamic of the mobile mass motion.

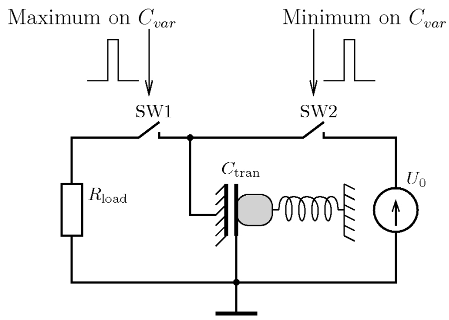

Figure 1. Simplified conditioning circuit used for the modeling experiment. R_{load}=1Ohm

The resonator is submitted to a sinusoidal external vibration with frequency ω_f equal to the natural mechanical resonance frequency of the resonator. The acceleration amplitude A_{ext} changes slowly over time. Such a set-up allows a demonstration of the evolution of the system behavior for different external vibration magnitudes. An optimal operation of the system corresponds to a periodic quasi-sinusoidal motion of the resonator's mass at the frequency of the external vibrations. The numeric parameters of the system are given in table 1.

Experimental results and discussions

Fig. 2 presents the plots of the external acceleration ramp, the observed displacement of the mobile mass and zoomed plots highlighting different operation modes. For the zoomed plots, the pulses corresponding to events of detection of maximum on C_{var} values are presented. They are useful to highlight the regularity of the operation mode: one and only one max (and min) detection by period happens in a regular periodic mode.

The normal operation mode is observed on the zoom subplots 2: there is only one max detection over each period, and the existing theory of the constant-charge energy harvesting is valid only for this mode (concerning the harvested power, the transducer voltage evolution, etc., [4]). However, the three other modes are very different and are specific to a range of the external acceleration magnitude. In the next three subsections we consider each of them.

1) High-amplitude instability (subplot 4). To understand the high-amplitude instability, one should consider the dynamic of the mobile mass when the latter approaches the closest position to the fixed electrodes, X_{cl}. In this situation, the transducer's capacitance increases and the transducer is not biased. At X_{cl} position the maximum of the capacitance is detected, and the voltage U_0 is applied on the transducer. Note, that for the detection of a maximum of the transducer's capacitance, the latter should start to decrease, *i.e.* the mobile mass starts to move out from the fixed electrode. In this case, the transducer generates an attractive force $\frac{1}{2}U_0^2\varepsilon_0\frac{S}{(d_0-X_{cl})^2}$ and the restoring forces are generated by the spring and the external vibrations, *i.e.*, $kX_{cl}+\alpha m A_{ext}$. Here k and m are stiffness and mass of the resonator respectively, α is the coefficient between -1 and 1 whose value depends on the phase of the external vibrations when the mass position is equal to X_{cl}. The high-amplitude instability happens when, at this moment of the U_0 voltage application, the attractive force is superior to the restoring force. However, contrary to a case where the transducer is biased with a constant voltage, the mobile mass is not pulled on the fixed electrode. Indeed, under the action of the transducer's attractive force, the mobile mass starts to move toward the fixed electrode. But then the capacitance increases again, hence, a local minimum is detected and the conditioning circuit discharges the transducer so preventing it from a pull-in. The attractive force disappears, and the transducer moves away from the fixed electrode. The capacitance decreases, hence a maximum of C_{var} is detected, the voltage U_0 is applied again, and the described process is repeated. This behavior is observed on the subplot 4 of the fig. 1: One can see that the mobile mass remains for a long time on a position close the fixed electrode, and during this time interval, many maximum detections happen.

If the conditioning circuit is ideal (no delay in the max/min detection, instantaneous charging of C_{var}), the C_{var} min/max detections happen with infinite frequency. In reality, in this case the delays in the conditioning circuit define the actual dynamic of the system, which is chaotic and is very different from the well-studied pull-in dynamic, as can be seen on subplot 4.

2) Middle-amplitude instability (subplot 3). The simulation highlights that the regular behavior of a constant-charge VEH with gap-closing transducer (as in subplot 2) becomes unstable when X_{cl} is even less than the value at which the attractive force exceeds the restoring forces. As can be observed on the subplot 3, in this mode the 2nd and higher harmonics impact strongly the response of the resonator, the dynamic starts to be less regular and the efficiency of the energy harvesting may decreases.

3) Low amplitude instability (subplot 1). Another manifestation of instability in electrostatic VEH happens at very weak amplitudes of external vibrations. On subplot 4 it can be seen that the mobile mass remain a long time at the extreme positions, and during this time, many maximum detection events happen. To our knowledge, such a phenomenon has never been reported in previous studies.

The second part of the article presents the theoretical tools allowing an analytical description of the behavior presented in fig. 2.

III. THEORETICAL DESCRIPTION OF THE OBSERVED INSTABILITY MODES

The proposed analysis of the observed phenomena is based on the analytical model of vibration energy harvesters proposed in [6]. This analytical tool is based on the harmonic balance method limited to the first (fundamental) harmonic, and is valid for narrow-band resonator (with Q>10).

Low limit of A_{ext} value required for stable operation

1) Newtonian law for harmonic 0. The existence of a low limit of A_{ext} required for a stable quasisinusoidal periodic operation of VEH can be highlighted by considering the coupling between the 0 and 1 harmonics of the mobile mass displacement. As shown in [6], in the considered case the transducer generates a constant force F during one half of the period:

$$F=\frac{1}{2}U_0^2\varepsilon_0\frac{S}{(d_0-X_{cl})^2}, \qquad (2)$$

and a zero force during the another half of the period. Hence, the average (0 harmonic) force is *F/2*. Writing down the second Newtonian equation for the 0 harmonic, we have:

$$kX_{av} = \frac{F}{2} \text{ and } X_{av} = \frac{F}{2k}, \qquad (3)$$

where X_{av} is the average position of the mobile mass. However, it is evident that X_{av} should be not less than X_{cl}, hence the valid closest position of the mass X_{cl} is given by the inequality.

$$\frac{1}{4k} U_0^2 \varepsilon_0 \frac{S}{(d_0 - X_{cl})^2} \le X_{cl} \qquad (4)$$

The solution of this inequality is an interval [X_1, X_2]. X_1 gives the minimal closest position X_{cl} for which the system can operate in a stable mode for a given transducer geometry, *k* and U_0. It is impossible to find a close expression defining it. However, it is easy to find it through a numeric method.

2) Newtonian law for harmonic 1. This subsection uses the study reported in [6] which described the regular behavior of electrostatic VEH through the first harmonic method. This analysis introduced a mechanical impedance of the transducer at the first harmonic, defined as $\Psi_t = -\frac{F_t^\omega}{V}$. Here F_t^ω is the complex amplitude of the first harmonic of the force generated by the transducer, *V* is the complex amplitude of the velocity of the mobile mass. For the considered VEH, the transducer has the impedance given by

$$\Psi_t = \frac{1}{\pi} \frac{U_0^2 C_{\max}^2}{\varepsilon_0 S} \frac{1}{\omega X^\omega}, \qquad (5)$$

where C_{max} is the value of the transducer capacitance measured at the position X_{cl}, X^ω is the amplitude of the mobile mass displacement. X^ω can be expressed through X_{cl} and X_{av}, hence, the impedance is a function of X_{cl}. Now, the second Newtonian law for the first harmonic can be written:

$$\left|\Psi_t + \Psi_r\right| = \frac{mA_{ext}}{\omega X^\omega}, \qquad (6)$$

where Ψ_r is the mechanical impedance of the resonator, which is equal to the damping constant if the vibration frequency is close to the resonance.

This equation relates X_{cl} and A_{ext}. Since the inequality (4) transformed into an equality is valid for X_1 corresponding to the minimal X_{cl} at which the behavior is stable, injecting (4) into (6) gives for $A_{ext\,min}$:

$$A_{ext\min} = \frac{4}{\pi} \omega^2 X_1 \approx \omega^2 X_1 \qquad (7)$$

This equation gives a very simple requirement on the external vibration magnitude: The displacement amplitude of the external vibration should be above X_1.

This result is in a perfect agreement with the modeling experiment presented in fig. 2.

Limit of A_{ext} between high amplitude and middle amplitude unstable modes

As we said in the sec. 2, the high amplitude instability happens at the same conditions as the pull-in in the constant-voltage biased transducer, i.e. when

$$\frac{1}{2} U_0^2 \varepsilon_0 \frac{S}{(d_0 - X_{cl})^2} \ge kX_{cl} + \alpha m A_{ext}. \qquad (8)$$

Since the mechanical impedance of the transducer is real, and since we consider the system at the resonance, the external force ($ma_{ext}(t)$) and the displacement of the mobile mass are shifted by $\pi/2$, hence, α=0. Similarly with the inequality (4), the minimal X_{cl} at which the system enters into the high amplitude instability mode is given by the equation corresponding to (8). Note that this value corresponds to the instable equilibrium position of the mass when the transducer is biased with a constant voltage U_0. (called $X_{eq.inst.}$). This value can only be obtained by solving the equation numerically. For the studied system it is 12 m: Indeed, on the fig. 2, the large-amplitude instability is observed for larger X_{cl}.

Limit of A_{ext} between stable mode and middle amplitude unstable modes.

The middle-amplitude instability at which a periodic but non-sinusoidal behavior is observed, is a complex phenomenon related with the nonlinearity of the circuit. It is difficult to explain "qualitatively". We propose the following explanation: This mode is related with the fact that the position X_{cl} becomes too close to the fixed electrode, and that at this point, the high harmonics of the transducer's force can't be filtered by the resonator passband characteristic and starts being dominant in the circuit behavior.

The theory reported in [6] offers a sufficient condition for stability of the regular mode (subplot 2). Obviously, when A_{ext} increases and the middle-amplitude instable mode appears (subplot 3), the regular mode (subplot 2) becomes unstable. Hence, the condition given in [6] provides a necessary criterion for appearance of the unstable mode at the given amplitude of vibration. This condition is formulated as:

$$\left|\frac{d\left|\Psi(X)\right|}{dX}\right|_{X=X^\omega} \ge \left|\frac{\Psi(X^\omega)}{dX^\omega}\right|, \qquad (9)$$

where $\Psi(X)$ is the total mechanical impedance of the system ($\Psi_t + \Psi_r$). This condition does not directly depend on the external vibration magnitude, but is indirectly related with it through X^ω. When applied to our system, the criterion (9) gives 8.7 m for the maximal X_{cl} at which the system is stable. Above this X_{cl}, the system enters in the middle amplitude instability mode. This is in a good agreement with the simulation. However, the criterion (9) provides only a necessary, not sufficient condition for appearance of the middle amplitude instability mode. Hence, in general, the maximal X_{cl} and X^ω predicted with it are pessimistic: The dynamic can be stable and regular event for larger values of X_{cl} and X^{ω}. Further investigations are needed in order to find a necessary and sufficient criterion.

IV CONCLUSION

This study provided an insight in the dynamic behavior of capacitive VEH using a gap-closing capacitive transducer. The issues related with stability were deeply investigated. It was discovered that depending on the magnitude of external vibrations, three different kinds of pathologic behavior is possible: at low amplitude, at large amplitude and at middle amplitude. None of this behavior is similar with what has been observed for constant voltage biased capacitive transducer. A theoretical insight allowing a quantitative characterization of the highlighted instability phenomena is exposed in the paper.

V ACKNOWLEDGMENTS

This project has been funded by the French National Agency of Research (ANR) through the project ANR/ARPEGE 08-SEGI-019.

REFERENCES

[1]. P. Basset et al., "A batch-fabricated and electret-free silicon electrostatic vibration energy harvester", J. of Micromech. Microeng., vol. 19, n. 11, 2009

[2]. F. Najar et al., Dynamics and Global Stability of Beam-based Electrostatic Microactuators, Journal of Vibrations and Control, vol. 16, no. 5, April 2010

[3]. F. M. Alsaleem et al., On the nonlinear resonances and dynamic pull-in of electrostatically actuated resonators, Journal of Mircromech. Microeng., vol. 19, n. 4, April 2009

[4]. S. Meninger et al., "Vibration-to-electric energy conversion", IEEE transaction on very large scale integration systems, 9(1): 64-76, February 2001

[5]. D. Galayko et al., "AMS modeling of controlled switch for design optimization of capacitive vibration energy harvester", IEEE BMAS Conference, San José, CA, USA, Sept. 2007

[6]. D. Galayko, P. Basset, A General Analytical Tool for the Design of Vibration Energy Harvesters Based on the Mechanical Impedance Concept, IEEE TCAS I, vol. 58, num. 2, February 2011

Table 1. Parameters of the modeled system

Mass, m, kg	Stiffness, k, Nm^{-1}	Damping constant, , Nsm^{-1}	Quality factor, Q	Resonance frequency, f, Hz	Transducer's gap, d_0, m	Transducer area, S, m^2	U_0, V
$100{\cdot}10^{-6}$	150	$1.0{\cdot}10^{-3}$	40	194.9	$20{\cdot}10^{-6}$	$10^{-2}\times{\cdot}10^{-2}$	15

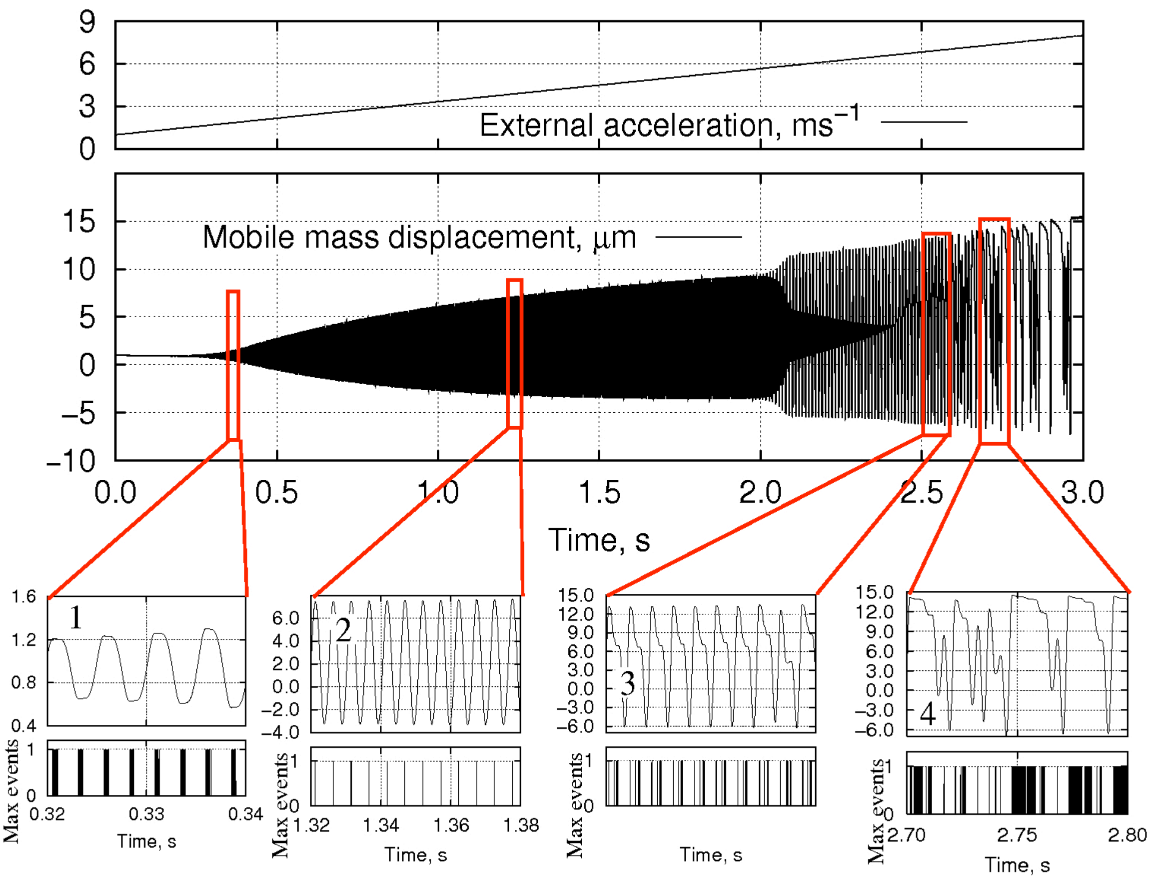

Figure 2. Dynamics of the VEH and zooms on different stability modes : 1) low amplitude instability, 2) stable regular mode, 3) middle amplitude instability, 4) high amplitude instability